

Lower Limb Prosthetics using Optimized Deep Learning Model – a Pathway Towards SDG Good Health and Well Being

Prakash. S^{1,*} , Jeyasudha. M² , Priya. S³ , M. Batumalay⁴ 

^{1,2}Department of Electrical and Electronics Engineering, Bharath Institute of Higher, Education and Research, Chennai, Tamil Nadu, India

³AMET University, Kanathur, Chennai, Tamil Nadu, India

⁴Faculty of Data Science and Information Technology, INTI International University Nilai, Malaysia

(Received: May 30, 2024; Revised: June 21, 2024; Accepted: July 4, 2024; Available online: August 5, 2024)

Abstract

This research article aimed at revolutionizing prosthetic leg technologies to enhance accessibility, affordability, and environmental sustainability. With a focus on addressing the diverse needs of amputees globally, the program integrates principles of eco-design, community engagement, technological innovation, and policy advocacy to foster inclusive and resilient societies which leads to the attainment of Sustainable Development Goal (SDG) Good Health and Well Being. Lower Limb Prosthetics of Activity Recognition is an innovative field combining prosthetic technology and activity recognition systems. The challenge of activity recognition in lower limb prosthetics to optimize the performance and responsiveness of mock limbs. In this work, the problem is overcome by using the Optimized deep learning technique, which improves activity recognition in lower limb prosthetics. The proposed methodology consists of (1) Pre-processing (2) Feature extraction (3) Feature classification. The collected images are pre-processed via improved wavelet demonizing and Empirical mode decomposition. From pre-processed data, the features are extracted using an improved sliding window method. The obtained extracted features are moved on to the Feature classification process. The classification process is done by the Optimized Long short- term memory. They are designed to better capture dependencies and patterns in sequential data, which makes them highly effective for tasks involving time series, natural language processing and other sequential data problems. Optimization can be done by proper data preprocessing and tuning the data from data extraction. The weight of the LSTM model is optimized to improve the performance of this model by the improved Black Window Optimization Algorithm. The main contributions of the paper are to obtain the best classification accuracy, an optimized LSTM model is introduced in this paper, and the weight of the LSTM model is enhanced by the improved Black Window Optimization algorithm. It improves the performance of the proposed system.

Keywords: Lower Limb Prosthetics, Activity Recognition, Improved Black Window Optimization, Optimized LST, Process Innovation

1. Introduction

Many natural systems inspire humans to lead technical advancements. The field of biomedical engineering has advanced recently, allowing prosthetic limbs to be developed that mimic the range of motion of amputees [1]. Individuals regularly have their lower limbs amputated; prosthesis help people live better by giving back the mobility of their missing limbs. Losing one or multiple structural elements of the human organism, regardless of the cause, is commonly referred to as amputation. Common causes of limb loss include surgical amputations, certain diseases, and traumatic traumas [2].

Prosthetic limbs have been used since ancient times. Archaeological evidence suggests that early prosthetic devices were crafted by the Egyptians around 3000 BCE. These early prosthetics were typically made of wood and leather. In recent decades, advancements in materials science, robotics, and bioengineering have revolutionized prosthetic technology. Carbon fiber, microprocessors, and advanced sensor technology have enabled the creation of highly sophisticated prosthetic limbs that closely mimic the function and movement of natural limbs. Companies and researchers continue to push the boundaries of what is possible, with innovations such as mind-controlled prosthetics and osseointegration (the surgical implantation of prosthetic devices directly into the bone) becoming increasingly common.

*Corresponding author: Prakash. S (prakash.eee@bharathuniv.ac.in)

 DOI: <https://doi.org/10.47738/jads.v5i2.178>

This is an open access article under the CC-BY license (<https://creativecommons.org/licenses/by/4.0/>).

© Authors retain all copyrights

Lower limb prosthetics involves designing and constructing artificial limbs to substitute amputated or lost lower limbs, giving those who have lost limbs their mobility back. These prostheses are essential in helping amputees regain their freedom and participate fully in everyday life [3]. Enhancing the user encounter and biomechanics are the main goals of recent developments in lower limb prosthesis. Innovations include powered prostheses with intelligent control systems, allowing for more natural and adaptive movements. Such prosthetics often integrate sensors and microprocessors to detect the user's gait intent, adjusting the prosthesis's behaviors accordingly [4]. The Materials and design play a pivotal role in ensuring comfort and durability. The interface among the prosthesis and residual limb, known as the prosthetic socket, is manufactured to provide an accurate fit and reduce pain. Additionally, advancements in socket technology aim to reduce pressure points and enhance overall comfort [5]. The field of lower limb prosthetics also explores the integration of robotics and artificial intelligence to enable prostheses that mimic human-like movements and respond to varying terrains. Research continues to refine these technologies, considering user-specific needs and preferences [6].

The development of lower limb prosthesis improves the general health and quality of life for those who are experiencing limb loss in addition to restoring physical capacities. Through continued research and development, amputees worldwide are looking for methods to enhance the prosthetic limbs' flexibility, accessibility, and smooth integration into their everyday lives [7]. Activity Recognition of Lower Limb prostheses entails the identification and classification of the movements and activities performed by individuals donning lower limb prostheses. The achievement is rendered feasible by the employment of cutting-edge technology, encompassing sensors and algorithms derived from the principles of machine learning [8]. Intending to improve user-prosthetic device interaction, the research seeks to provide more natural control and flexible responses. Walking and stair climbing are two examples of lower limb activities that the system can discriminate between by examining data such as surface electromyography (sEMG). The creative method advances the creation of intelligent prosthetic devices, enhancing their general usability and functionality for people who have lost limbs [9], [10].

Lower limb prosthetics with activity recognition is a cutting-edge field that combines advancements in prosthetic technology with intelligent systems to enhance the mobility and interaction of individuals with limb loss [11]. Activity recognition involves the identification and interpretation of various lower limb movements, enabling prostheses to adapt dynamically to the user's intentions [12]. The impact of lower limb prosthetics with activity recognition extends beyond basic mobility. Users can engage in a broader range of activities with increased confidence and reduced cognitive effort [13]. The navigating varied terrains or engaging in specific tasks like climbing stairs, the prosthetic adapts seamlessly to the user's needs. The integration of artificial intelligence and advanced sensor technologies holds the promise of further refining lower limb prosthetics with activity recognition [14]. This article proposes a comprehensive way to deal with prosthetic leg improvement that focuses on friendly value, ecological stewardship, and innovative headway. The main contributions of the paper are as follows:

- 1) To enhance the extraction process, the improved sliding window technique is used in this paper, the effectiveness of this technique is demonstrated through improved precision and concert of lower limbs activity.
- 2) To obtain the best classification accuracy, an optimized LSTM model is introduced in this paper, the weight of the LSTM model is enhanced by the improved Black Window Optimization algorithm. It improves the performance of the proposed system.

2. Literature Study

This section provides a review of a few of the more recent research studies that pertain to the Lower Limb Prosthetics of Activity Recognition. The researchers Vijayvargiya et al. [15] investigated the possibility of using wearable sensors, more sEMG sensors, to identify actions that occur in the lower limbs. Wavelet denoising and overlapping windowing were the methods that the author suggested for hybrid deep learning models. These methods were used to eliminate noise and segment signals. The performance indices demonstrate that these models perform better than individual models, which substantiates their effectiveness in identifying actions involving the lower limbs. Zhang and Tao [16] analyzed the disparities in scope, description of the research, availability of data, and incorrect citations. They addressed the Pattern recognition of Lower Limb Motion Based on a Convolutional Neural Network (CNN) and detailed the findings of their investigation. It discussed the utilization of sEMG signals and CNN for the purpose of evaluating the

motion pattern of the lower limb. It drew attention to the fact that assistive technologies like exoskeletons require precise motion identification, and it compared the accuracy of the proposed method to that of more conventional approaches.

According to Cimolato et al. [17], a cutting-edge neuromusculoskeletal (NMS) model that makes use of machine learning techniques is currently being developed for lower limb prosthetics. This model is able to efficiently overcome the constraints that are associated with electromyography-driven models. Despite the fact that several electrodes are required, the particular model makes use of wearable sensors to estimate joint torque in order to create a smooth interface between human control and wearable robotics. In the year 2021, Wang et al. [18] presented their findings regarding the estimation of human lower limb movement using a multi-branch neural network rather than sEMG at the time. In order to analyze the movement of the lower limbs that was formed on sEMG signals in a sequential manner, the researchers designed a method. This research has the potential to make significant contributions to the field of biological signal processing and control.

With the assistance of machine learning, Zhou et al. [19] explored the process of accurately recognising various forms of lower limb ambulation by utilizing surface electromyography and motion data. A method that combines these two types of data is proposed by the researchers as a means of improving the accuracy of recognition. This project is intended to make a significant contribution to the field of gait analysis and assistive technologies for those who have difficulties moving around due to mobility restrictions. During the year 2020, Hussain and colleagues [20] investigated the utilization of sEMG signals for the purpose of intent identification in lower limb prostheses. An innovative approach for extracting features is proposed, which makes use of bispectrum magnitude and unsupervised feature reduction. This method improves the performance of activity recognition. Both the great accuracy and the durability of the method in a variety of prosthesis kinds point to the possibility that it could be used to regulate wearable devices. In the year 2021, Wang [21] provided an explanation that the research makes use of a CNN deep learning system to determine the motion intention of lower limb prostheses, hence enhancing control performance. It is possible for the model to attain a recognition rate of 98.2% over a variety of terrains, which enables smooth transitions between different movement modes. It is necessary to conduct additional study in order to enhance the accuracy of recognition for various movement types.

The neural network-based approach for assessing lower limb motion intention while using sEMG data was described by Li et al. [22] in the year 2022. An improved prediction accuracy is achieved by the utilization of a fuzzy wavelet neural network (FWNN) in conjunction with a zeroing neural network (ZNN) in the model. Additionally, it compares simulations by utilizing sEMG signals and motion data from seven muscles while the individual is walking. In addition to underlining the significance of sEMG signals, the model provides a theoretical foundation for rehabilitative robot interface and provides an accurate estimation of human motion intention. An efficient weighted feature technique was presented by Wang et al. [23] for the purpose of increasing the rate of appreciation for lower limb motions based on sEMG. The advanced genetic algorithm-support vector machine (IGA-SVM) was developed to solve the problem of the genetic algorithm choice operator accidentally falling into the local optimal solution. After putting the proposed method through its paces on six distinct lower limb motions, the results showed a regular identification rate of 94.75%. The method demonstrates how to recognize activities involving the lower limbs. In contrast, Vijayvargiya et al. [24] provided an explanation of the WD-EEMD technique that was introduced for the purpose of classifying lower limb activities by utilizing sEMG data. The utilization of empirical mode decomposition in conjunction with wavelet denoising is employed in order to eradicate unwanted signals and noise. A linear discriminant analysis classifier is used to test the technique, and it obtains a high level of classification accuracy that is satisfactory. Applications connected to the identification of lower limb activity also make use of sEMG signals. These applications include human-machine interface and neuromuscular disease diagnosis situations.

The challenge of activity recognition in lower limb prosthetics to optimize the performance and responsiveness of mock limbs. In this work, the problem is overcome by using the Optimized deep learning technique, which improves activity recognition in lower limb prosthetics. The proposed methodology consists of Pre-processing, Feature extraction and Feature classification. The collected images are pre-processed via improved wavelet denoising and Empirical mode decomposition. From pre-processed data, the features are extracted using an Improved sliding window method. The obtained extracted features are moved on to the Feature classification process. The classification process is done by the

Optimized LSTM method. The weight of the LSTM model is optimized to improve the performance of this model by the improved Black Window Optimization Algorithm.

Developing lower limb prosthetics through optimized deep learning models represents a significant stride towards achieving SDG 3: Good Health and Well-being. By leveraging advanced technologies like deep learning, prosthetic limbs can be tailored more precisely to individual needs, enhancing comfort, mobility, and overall quality of life for amputees.

3. Methodology

Lower Limb Prosthetics of Activity Recognition is an expanding field that combines advanced prosthetic technology with activity recognition systems to improve the functionality and usability of prosthetic limbs. By accurately detecting and classifying different activities, such as walking, running, or climbing stairs, individuals can experience a more seamless integration of their prosthetic limb into their daily lives. This can ultimately lead to increased independence and overall well-being for amputees. Figure 1 shows overall design for the proposed model. In this research work, the lower limb prosthetics of activity recognition is done using a deep learning model developed by the mentioned stages for the subsequent flow which includes comprehensive data acquisition flowed by elaborated pre-processing technique. The pre-processing includes improved wavelet diagnosis and empirical mode decomposition. Next, would-be rigorous feature extraction procedure to improve sliding window and time domain feature. Finally, advanced feature classifier mechanism will optimize the LSTM.

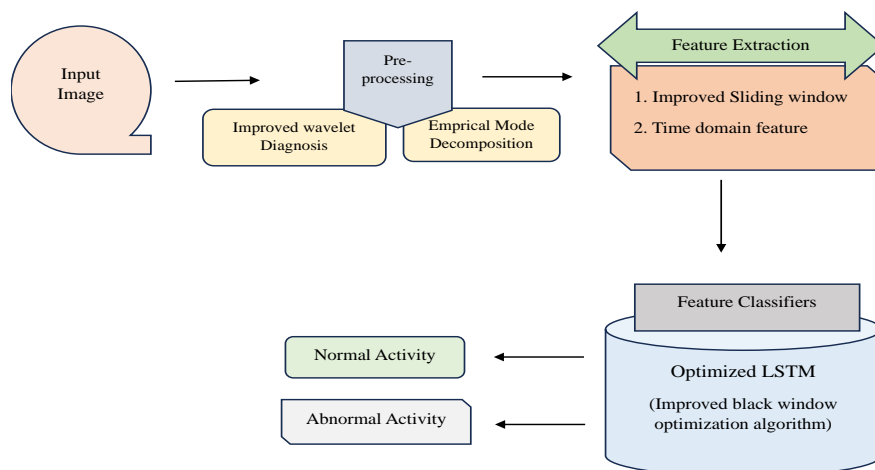


Figure 1. Overall design for the proposed model

3.1. Data Acquisition

Images are used to acquire the raw data that is being collected. The process of retrieving a picture from an external source for the purpose of further processing is referred to as image acquisition in the field of image processing. Since there is no action that can be performed prior to the acquisition of a picture, this step is always the foundational one in the workflow. In order to categorize lower limb activity, the study makes use of datasets from the University of California, Irvine that are accessible to the public. There are 22 volunteer participants who are at least 18 years old, and only one of them is in good physical condition. The remaining people have knee deformities. When lower limb activities are being performed, the focus of the investigation is on the influence that EMG signals have on the muscles of the lower limbs [16]. Four surface electrodes and a goniometer that was mounted to the exterior of the knee joint were utilized in order to acquire the necessary data. Using a Bluetooth adapter, the data was transferred to the Datalog programme in real time after being stored on the computer directly from the MWX8 storage which was connected to the computer. This study focuses solely on the sEMG signals during lower limb movements in order to investigate the influence that EMG signals have on the muscles of the lower limbs. When it came to healthy individuals, there was no previous case history that was discovered relating knee pain or damage.

3.2. Pre-processing

The Image from the data acquisition is pre-processed by Improved Wavelet Denoising and empirical mode decomposition. In Pre-processing the lower limb activity recognition involves refining raw data before analysis. Effective pre-processing enhances the accuracy of deep learning models for recognizing and classifying lower limb activities based on sensor data. Wavelet denoising and EMD are used for preprocessing because they offer effective methods for removing noise and decomposing signals into more manageable components.

3.2.1. Improved Wavelet Denoising

The procedure of performing wavelet denoising encompasses the application of a threshold to the wavelet coefficients to mitigate noise while preserving the crucial constituents of a signal and it is denoted as per the formula (1):

$$R(g) = c(g) + \sigma(g) \tag{1}$$

Where, $R(g)$ denotes the noisy signal, $c(g)$ be the ideal signal and $\sigma(g)$ be the noise intensity.

Threshold Denoising: The role of the wavelet threshold is crucial in determining which wavelet coefficients are noise [25]. The threshold magnitude directly affects the quality of the reconstructed signal. The signal is created using low-frequency constants from layer P then high-frequency constants from layers 1 to P. The key aspect is choosing the threshold and quantifying wavelet constants after threshold, as linked for denoising outcome.

The execution of the thresholding operation is an essential and pivotal procedure in the enhancement of wavelet denoising. Among the selection of thresholding functions, notable examples encompass soft thresholding and hard thresholding. The function for conventional hard threshold denoising function is denoted as per the formula (2):

$$v'_{t,u} = \begin{cases} v_{t,u} & |v_{t,u}| \geq \lambda \\ 0 & |v_{t,u}| < \lambda \end{cases} \tag{2}$$

The function for conventional soft threshold denoising function is denoted as per the Formula (3):

$$v'_{t,u} = \begin{cases} \text{sign}(v_{t,u}) \times (|v_{t,u}| - \lambda) & |v_{t,u}| \geq \lambda \\ 0 & |v_{t,u}| < \lambda \end{cases} \tag{3}$$

Where λ be the threshold and $v'_{t,u}$ is the new wavelet constants. In soft thresholding function, there is constant variation among $v'_{t,u}$ and $v_{t,u}$ when $|v_{t,u}| \geq \lambda$.

3.2.2. Empirical Mode Decomposition (EMD)

EMD is the methodology employed for scrutinizing data that entails breaking down a signal into intrinsic mode functions (IMFs) in order to apprehend its inherent oscillatory modes. This technique is especially efficacious in analysing non-stationary signals, as it affords a focused and adaptable depiction of signal components, all the while abstaining from dependence on pre-established basis functions.

- 1) The higher $q(x)$ and lower $i(x)$ covers are formed with interruption of all local maximum then minimum for $g(x)$.
- 2) A running mean envelope $p(x)$ is calculated using $p(x) = \frac{q(x)+i(x)}{2}$
- 3) The mean cover is subtracted from signal, that bounces $u(x) = g(x) - p(x)$.
- 4) The $u(x)$ verifies the IMF condition its entire length must be either equal or varies by 1. The mean value for $u(x)$ be zero.
- 5) If $u(x)$ not fulfil the condition for IMF, $g(x)$ is substituted with $u(x)$ then selecting is sustained till the signal gotten meet the situations. The selecting process can also be ended if $u(x)$ is monotonic function. The incentive signal $g(x)$ gained through summation for IMFs then denotes as per the Formula (4):

$$g(x) = \sum_{p=1}^{P-1} \text{IMF}_p(x) + s_p(x) \tag{4}$$

where s_p is enduring term later moving $P - 1$ IMFs. Though, EMD encounters challenge with regard to the frequent occurrence of mode mixing, which stems from its susceptibility to noise. To moderate this issue, the method of noise-assisted data analysis, known as ensemble EMD, was introduced. It characterizes the IMFs as the mean value obtained from a set of experiments. A white noise series with equal typical variation is extra to targeted data denoted as per the Formula (5):

$$g_p(x) = g(x) + l_p(x) \tag{5}$$

where $l_p(x)$ is p th white noise series further to $g(x)$, then $g_p(x)$ is noise-supplementary signal.

3.3. Feature Extraction using Improved Sliding Window Technique

The processed data from pre-processing are given to the feature extraction process. Feature extraction in lower limb activity recognition involves identifying and extracting relevant patterns or characteristics from sensor data, such as accelerometers or surface electromyography signals. Common features include temporal and frequency-domain attributes, statistical measures, or wavelet coefficients. The improved sliding window method is used for feature extraction in time-series data and other sequential data to enhance the accuracy and efficiency of identifying and capturing relevant patterns and characteristics.

The improved sliding windowing technique is employed for feature extraction, in contrast to considered whole signal at once, because of its stochastic nature. The procedure is used for segmentation, either adjacent or overlapped [24]. The outcomes demonstrate the accuracy of categorization is higher for the overlain windowing strategy compared to the adjacent or disjunct windowing scheme. Data stability during feature extraction is ensured by segmenting the data into brief windows. Each temporal series was divided into ideal segments or sub-frames using the overlapping windowing technique in this investigation.

The feature extraction process exhaustively explained as trails: First, points $R_1(I_1, A_1, X_1)$, $R_2(I_2, A_2, X_2)$, and $R_3(I_3, A_3, X_3)$ were placed in primary window. Using time X_2 for point $R_2(I_2, A_2, X_2)$ as an index, the variance among $R_1(I_1, A_1, X_1)$ and $R_3(I_3, A_3, X_3)$ can be calculated as $R'_2(I'_2, A'_2, X_2)$. If spacio temporal detachment H is under the threshold, then comparative azimuth angle from R_1 to R_2 were recalculated and termed E_1 . The R_1 sequence is denoted as E_0 . The alteration ΔE among E_1 and E_0 must be below the intended angle threshold. If this form is fulfilled, R_2 can be erased. This should be below the considered angle threshold as per the Formula (6), Formula (7), Formula (8), Formula (9).

$$\Delta k = X_k - X_h \tag{6}$$

$$\Delta d = X_d - T_h \tag{7}$$

$$A'_k = A_h + \frac{\Delta k}{\Delta d} (A_d - A_h) \tag{8}$$

$$I'_k = I_h + \frac{\Delta k}{\Delta d} (I_d - I_h) \tag{9}$$

where A be AIS latitude, I is AIS longitude, X be AIS time, Δk denotes time passed from primary point to check point, also Δd is time passed from the starting point to the end point. Muscle contraction, activity detection, and onset detection all make use of time-domain properties. Neurological problems and muscular exhaustion are detected using frequency domain characteristics. Table 1 shows the mathematical expression of Mean, Median, RMS, ZC, SSC, DASVD, variance, Average Amplitude Change, Skewness and kurtosis

Table 1. mathematical expression of Mean, Median, RMS, ZC, SSC, DASVD, variance, Average Amplitude Change, Skewness and kurtosis.

| Metrics | Description | Mathematical expression |
|------------------------|--|---|
| Mean | The arithmetic means of a collection of two or more numerical values. | $\mu = \frac{1}{L} \sum_{k=1}^L u_k $ |
| Root Mean Square (RMS) | The statistical measure that calculates square root for average of the squared values within the dataset. | $\sqrt{\frac{1}{L} \sum_{k=1}^L u_k ^2}$ |
| Zero Crossing (ZC) | The signal processing concept identifies points in a signal where the amplitude changes its sign. It refers to instances where the signal crosses the zero axis. | $\sum_{k=1}^{L-1} f(u_k)$ Where |

$$f(u_k) = \begin{cases} 1 & \text{if, } (u_k > 0 \text{ and } u_{k+1} < 0) \\ & \text{or } (u_k < 0 \text{ and } u_{k+1} > 0) \\ 0 & \text{otherwise} \end{cases}$$

$$\sum_{k=1}^{L-1} f(u_k)$$

Where

$$f(u_k) = \begin{cases} 1 & \text{if, } (u_k > u_{k-1} \text{ and } u_k > u_{k+1}) \\ & \text{or } (u_k < u_{k-1} \text{ and } u_k < u_{k+1}) \\ 0 & \text{otherwise} \end{cases}$$

$$\sqrt{\frac{1}{L-1} \sum_{k=1}^{L-1} (u_{k+1} - u_k)^2}$$

$$\frac{1}{L-1} \sum_{k=1}^L (u_k)^2$$

$$\frac{1}{L} \sum_{k=1}^{L-1} |u_{k+1} - u_k|$$

$$Skew = \frac{1}{L} \sum_{k=1}^L \left[\frac{(u_k - \bar{u})}{\sigma} \right]^3$$

$$Kurt = \frac{1}{L} \sum_{k=1}^L \left[\frac{(u_k - \bar{u})}{\sigma} \right]^4$$

Slope Sign Change (SSC) Counting number of times slope for signal variations its sign and employed to capture variations and transitions in a signal, providing insights into its dynamic behavior.

Difference Absolute Standard Deviation Value (DASVD) An analytical statistical metric that evaluates the percentage difference among each data point and the mean to quantify the dispersion or variability of a group of values. A measure of how much data differ from the mean is the standard deviation, which must be calculated.

Variance The statistical measure quantifies degree for spread or dispersal in set of data points. The average squared deviation for each data point from the mean of the dataset.

Average Amplitude Change (AAC) Calculates the average absolute difference in amplitude between consecutive data points within a signal. It quantifies the overall change in signal amplitude over a specific duration.

Skewness The measurement for symmetry, or the absence thereof, is undertaken.

Kurtosis Whether the data exhibits heavy-tailed or light-tailed characteristics can be assessed through appropriate measures.

u_k is a sample of the signal. σ denotes Standard Deviation. L denotes the amount of data in the sample. u_k represents each data point μ be the average of the dataset.

3.4. Feature Classification Using Optimized Deep Learning Methods

Feature classification using optimized deep learning methods involves leveraging advanced techniques to categorize extracted features from data. The optimization process involves parameter tuning and efficient training, resulting in superior classification performance. This approach is pivotal in domains like lower limb prosthetics, where accurate feature classification is crucial for seamless integration and responsive control, ultimately improving the user experience. In this work, the optimized LSTM is used by improved black window optimization algorithm. The improved black window optimization algorithm (BWOA): The Improved Black Widow Optimization Algorithm signifies an ameliorated rendition of the BWOA, the bio-inspired optimization algorithm grounded on the predatory conduct of black widow spiders. The improved version likely incorporates refinements to the algorithm's exploration and exploitation mechanisms, aiming to enhance convergence speed and solution quality. These enhancements could include adaptive parameter tuning, modified updating strategies, or incorporation of additional heuristics for increased optimization.

3.4.1. Population Initialization

An algorithm's search range can be increased, its optimization level and convergence time can be accelerated, and its beginning population diversity can all help. The typical BWOA algorithm's development ability may be hampered by an unequal distribution of black widows resulting from random beginning population placements. These weaknesses can be made up for by the positives of the chaotic motion map, which include unpredictability, regularity, and

ergodicity. To minimize the drawbacks of arbitrary populace, initialize also to speed up merging, researchers [26] are increasingly employing traditional chaotic map patterns, such as logistic then sine maps, for population initialization in optimization algorithms. Chaotic maps, a subset of dynamical systems characterized by their sensitive dependence on initial conditions and deterministic yet unpredictable behavior, have several applications across various fields. The unique properties of chaotic systems, such as sensitivity to initial conditions and long-term unpredictability, provide advantages in scenarios requiring security, randomness, and complex dynamic behavior modeling.

For logistic and sine maps, the value frequency is not uniform across the interval [0,1]. The algorithm's optimization efficiency will be decreased by the logistic map's or sine map's non uniform traversal. Determining the ideal position is not desirable, particularly when the global optimal position lies outside of the search range. Consequently, a novel double chaotic map approach is implemented, represented by Formula (10). Better diversity and more even distribution of the initial particles produced by the double chaotic map in the search space can increase the algorithm's optimization efficiency.

$$\begin{cases} g_{u+1} = q \cdot g_u (1 - g_u) \\ j_{u+1} = \frac{\omega}{4} \sin(\pi \cdot j_u) \\ y_{u+1} = \text{mod}(g_{u+1} + j_{u+1}, 1) \end{cases} \quad (10)$$

where g_u, j_u then y_u include u -th chaotic number $\text{mod}()$ is the remainder function. The original position for black widow specific is indicated through y_{u+1} with linear alteration, as per the Formula (11).

$$\vec{g}_k = ia_k + (qa_k - ia_k) \times y_u + 1 \quad (11)$$

where qa_k and ia_k are top and bottom limits of search space correspondingly.

3.4.2. The Sine Guidance

The sine guidance approach is introduced for prevent the original algorithm's premature convergence and increase optimization effectiveness of algorithm. It allows the algorithm for slowly approach optimal solution while fully utilizing variance data among spider and optimal spot. Linear and spiral motion are the two ways that spiders move on their webs. A black spider uses spiral movement to get to the optimal location $\vec{g}_*(x)$ after learning information from a potential partner.

The research proposes the sine algorithm to improve spiders' movement strategy. Despite boosting convergence speed, it reduces diversity in the spider population and increases the likelihood of local optimization. The previous meta-heuristic algorithms, updates a search space's position while considering the golden section coefficient, enhancing optimization precision.

$$\begin{cases} g_k^{x+1} = g_k^x \times |\sin(S_1)| + S_2 \times \sin(S_1) \times |\lambda_1 \times R_*^x - \lambda_2 \times g_k^x| \\ \lambda_1 = b + (1 - \tau) \times a \\ \lambda_2 = (1 - \tau) \times b + \tau \times a \\ \tau = \sqrt{5} - 1/2 \end{cases} \quad (12)$$

where R_*^x be historical best spot and g_k^x denotes location of k -th individual in x -th iteration; S_1 and S_2 are accidental numbers; τ represents golden section number. Original defaulting values for b and a were examined to be $-\pi$ and π , individually. λ_1 and λ_2 were two coefficients found later presenting section coefficient. The standards of λ_1 and λ_2 were modernized as impartial function value deviations. The present value might also move closer to the desired value thanks to these factors that somewhat narrow the search field. Following the use of the sine search algorithm, the black widow spider's location updating equation during its online movement is denotes as per the Formula (13).

$$\vec{g}_k(x+1) \begin{cases} \vec{g}_*(x) - p\vec{g}_{s_1}(x) & \text{if } \text{rand} \leq 0.3 \\ \vec{g}_k \times |\sin(S_1)| + S_2 \times \sin(S_1) \times \dots & \\ |\lambda_1 \times \vec{g}_*(x) - \lambda_2 \times \vec{g}_k(x)| & \text{in other cases} \end{cases} \quad (13)$$

Every time the position is changed, the k -th spider that has moved for potential mate's spot in web will communicate by that person. Every individual spider can understand exactly how it differs from the ideal individual. Furthermore,

by varying parameters S_1, S_2, λ_1 and λ_2 , the spider individual's movement may be controlled in terms of both distance and direction. Reducing the search space gradually is possible. The algorithm's convergence speed and optimization efficiency may be greatly enhanced.

3.4.3. Reverse Differential Mutation Operator

Every subsequent iteration will see a significant decline in the demographic variety in the BWOA. This research presents Cauchy bary center reverse variance mutation technique for produce altered spiders. The method aims to increase population variety, broaden the search area, and keep the algorithm from entering a state of local optimization.

The reverse mutation in center of gravity is explicit as $(g_{1t} + g_{2t} + \dots + g_{Lt})$ be value of L spiders on t -th dimension, the number of populations be L then, the number of the dimensions be F . The center of gravity for spider population in t -th dimension is defined by Formula (14). The center of gravity for population is $Y_o = (Y_1, Y_2, \dots, Y_t, \dots, Y_F)$

$$y_t = \frac{g_{1t} + g_{2t} + \dots + g_{Lt}}{L} \quad (14)$$

The reverse solution for center of gravity int-th dimension equivalent to k -th spider is as per the Formula (15):

$$g_{nt} = 2 * \text{cauchy}(0,1) * Y_t - g_{kt} \quad (15)$$

By using the Cauchy mutation, the algorithm may more successfully prevent position recurrence, broaden its search field, and improve its capacity for global exploration.

The differentiated evolution algorithm, which repeats via methods of mutation, crossover, and choice, is based on the differential mutation operator. Population mutation is indicated by weighted sum for differences among any two randomly picked specific vectors on search space also individual vector chosen at random through third person as per the Formula (16).

$$g_{\text{new}_k} = g_{s1} + C. (g_{s2} - g_{s3}) \quad (16)$$

Where c is the scaling factor. g_{s1} , and $g_{s2} - g_{s3}$ were basis vector and the difference vector correspondingly.

The benefits for two previously mentioned mutation procedures are combined in a novel mutation operator known as the Cauchy bary center reverse differential mutation operator, which places mutant spider close to modern population's center of gravity. The mutation operator expressed as per the Formula (17).

$$G_{\text{new}} = Y_o + C * (G_{p2} - G_{\text{worst}}) + C * (G_{\text{best}} - G_{p1}) \quad (17)$$

where Y_o denotes center of gravity for population. C be scaling factor. The two haphazardly chosen persons are arranged from excellent to terrible based on their fitness values, along with their corresponding individuals as $G_{\text{best}}, G_{p1}, G_{p2}, G_{\text{worst}}$. The above Eq (17) expression, which moves from the population's center of gravity toward the ideal individual, is correlated with fitness value for four chosen individuals of each mutant spider G_{best} .

The new mutation operator is not only arbitrary but also directional. IBWOA has a rapid convergence speed and can properly balance global exploration also local exploitation when novel hybrid strategies are applied to the algorithm for engineering-constrained optimization problems.

3.4.4. The Time Complexity

Let c be any optimization problem, and suppose the temporal complexity of determining important functional values is $N(C)$ without compromising generality. As a result, the BWOA's temporal complexity is expressed as $N(x_{\text{max}} \times l_{\text{Hr}} \times c)$. There are no newly nested loops for the IBWOA. The IBWOA's time complexity is $N(x_{\text{max}} \times l_{\text{Hr}} \times l_{\text{FD}} \times c)$, where l_{FD} be number of optimization problem valuations when Cauchy bary center reverse variance mutation operator is run, x_{max} denotes extreme number of iterations, and l_{Hr} represents number of spiders (populace size). When compared to original approach, the complexity increases marginally. Nonetheless, the algorithm's resilience, convergence speed, and search accuracy have all significantly increased.

3.4.5. The Space Complexity

The IBWOA's space complexity is the maximum amount of space that is considered at startup and may be used at any given moment. Consequently, the total space intricacy for IBWOA is $N(l_{HR} \times \text{dim})$, where dim be dimension for optimization problem.

LSTM: represents specific form of recurrent neural network structure meticulously devised to undertake the task of processing and forecasting sequences. LSTMs excel in capturing long-range depends on progressive data by maintaining memory cells with controllable forgetting and updating mechanisms. LSTMs find widespread application in the realm of time-series analysis, field of natural language dispensation, and discipline for speech recognition. They help to alleviate the vanishing gradient problem, which makes it possible to learn and model complicated temporal patterns effectively for a variety of applications and presented as per the Formula (18), Formula (19), Formula (20), Formula (21).

$$j_x = \sigma(V_j \cdot [o_{x-1}, V_x]) \quad (18)$$

$$h_x = \sigma(V_h \cdot [o_{x-1}, V_x]) \quad (19)$$

$$\widehat{o}_x = \tan m(V \cdot [h_x * o_{x-1}, V_x]) \quad (20)$$

$$o_x = (1 - j_x) * o_{x-1} + j_x * \widehat{o}_x \quad (21)$$

In an RNN, structure learning and parameter learning are done in two stages. The nodes receive membership functions in accordance with the input variable. The mean and variance are used to give the Gaussian membership function. Fire in space and temporal firing are used to assign membership functions that are just one dimension. All structure is learned ready to choose the appropriate time for each input to produce a rule and activate it with a firing strength greater than the threshold. The weight of the LSTM model is optimized to improve the performances of this model by the improved BWO.

4. Results and Discussion

This study introduces a model for the lower limb prosthetics of activity recognition using deep learning. This context compares the use of CNN, GRU and Optimized LSTM. To extract pertinent features, optimization model which is a fusion of Black window optimization, is employed. The presentation efficiency for recommended process is appraised through comparison it by various existing techniques in this section.

4.1. Performance Metrics

Several metrics were utilized to measure execution containing “Accuracy, Precision, F-Measure, Sensitivity, Specificity, negative prediction value (NPV), matthew’s correlation coefficient (MCC), false positive ratio (FPR), false negative ratio (FNR)”. Here we are measuring various performance metrics to compare it with existing system and to select best control algorithm for prosthetic leg.

The accuracy refers to proportion for properly secret data towards entirety for data present in log. The Accuracy is defined as:

$$\text{Accuracy} = \frac{XR + XL}{XR + CR + CL + XL} \quad (22)$$

By utilizing all the instances employed in the process of categorization, precision denotes description for complete quantity of authentic samples which adequately accounted for throughout the process of classification.

$$\text{Precision} = \frac{XR}{XR + CR} \quad (23)$$

The F-measure can be defined as the average of the recall rate and accuracy, focusing on consonant values.

$$F_{\text{Measure}} = \frac{2 \text{ Precision} \times \text{Recall}}{\text{Precision} + \text{Recall}} \quad (24)$$

The sensitivity measure is derived through the process of separating total number of positive consequences with ratio of accurate positive predictions.

$$\text{Sensitivity} = \frac{XR}{XR + CL} \tag{25}$$

The concept of specificity is deliberate as it is determined by proportion among number of acceptably predicted negative outcomes also complete number for negative outcomes:

$$\text{Specificity} = \frac{XL}{XL + CR} \tag{26}$$

The net present value (NPV) assesses the efficacy of an analytical examination or any other quantifiable measurement.

$$\text{NPV} = \frac{XL}{XL + CL} \tag{27}$$

Below is a depiction for binary variable suggestion measure referred to as MCC, which operates within a two-by-two framework.

$$\text{MCC} = \frac{(XR \times XL - CR \times CL)}{\sqrt{(XR + CL)(XL + CR)(XL + CL)(XR + CR)}} \tag{28}$$

The false positive rate is calculated by dividing the total number of negative events by the total number of negative events which are mistakenly classed as positive (false positives).

$$\text{FPR} = \frac{CR}{CR + XL} \tag{29}$$

The false-negative rate, also called the "miss rate," is the probability that a true positive might be missed by the test.

$$\text{FNR} = \frac{CL}{CL + XR} \tag{30}$$

4.2. Performance Evaluation

The performance metrics of three different neural network models: CNN, GRU, and Optimized LSTM. The accuracy metric reflects the overall correctness of the models. Table 2 shows the performance analysis for proposed versus existing classifier.

Table 2. Performance analysis for proposed Vs existing classifier

| | CNN | GRU | Optimized LSTM |
|--------------------|---------|---------|----------------|
| Accuracy | 0.96238 | 0.95023 | 0.98655 |
| Precision | 0.9689 | 0.95023 | 0.98712 |
| Recall | 0.96203 | 0.9575 | 0.98859 |
| F-score | 0.96774 | 0.9534 | 0.98485 |
| Specificity | 0.96667 | 0.9512 | 0.988 |
| Sensitivity | 0.96386 | 0.95082 | 0.98701 |
| MCC | 0.96591 | 0.95238 | 0.98805 |
| NPV | 0.96458 | 0.95161 | 0.98855 |
| FPR | 0.06341 | 0.07341 | 0.04341 |
| FNR | 0.05954 | 0.08954 | 0.03954 |

Table 2 shows the Optimized LSTM achieves the highest accuracy of 98.66%, surpassing both CNN and GRU. Precision, recall, and F-score provide insights into the models' ability to correctly classify positive instances. The Optimized LSTM exhibits superior precision (98.71%), recall (98.86%), and F-score (98.49%) compared to CNN and GRU. These values suggest the Optimized LSTM's proficiency in accurately recognizing positive occasions while minimizing false positives and false negatives. Specificity and sensitivity further elaborate on the models' performance in distinguishing between positive and negative instances. The Optimized LSTM demonstrates a high specificity of 98.80%, indicating its effectiveness in correctly identifying negative instances, and a sensitivity of 98.70%,

emphasizing its capability to detect positive instances. MCC, NPV, FPR, and FNR collectively assess overall typical performance. The Optimized LSTM consistently outperforms CNN and GRU across these metrics, with MCC at 98.81%, NPV at 98.86%, FPR at 4.34%, and FNR at 3.95%. So, it is best method of lower limb activity recognition by using this deep learning technique. Figure 2 depicts the classifier performance Analysis.

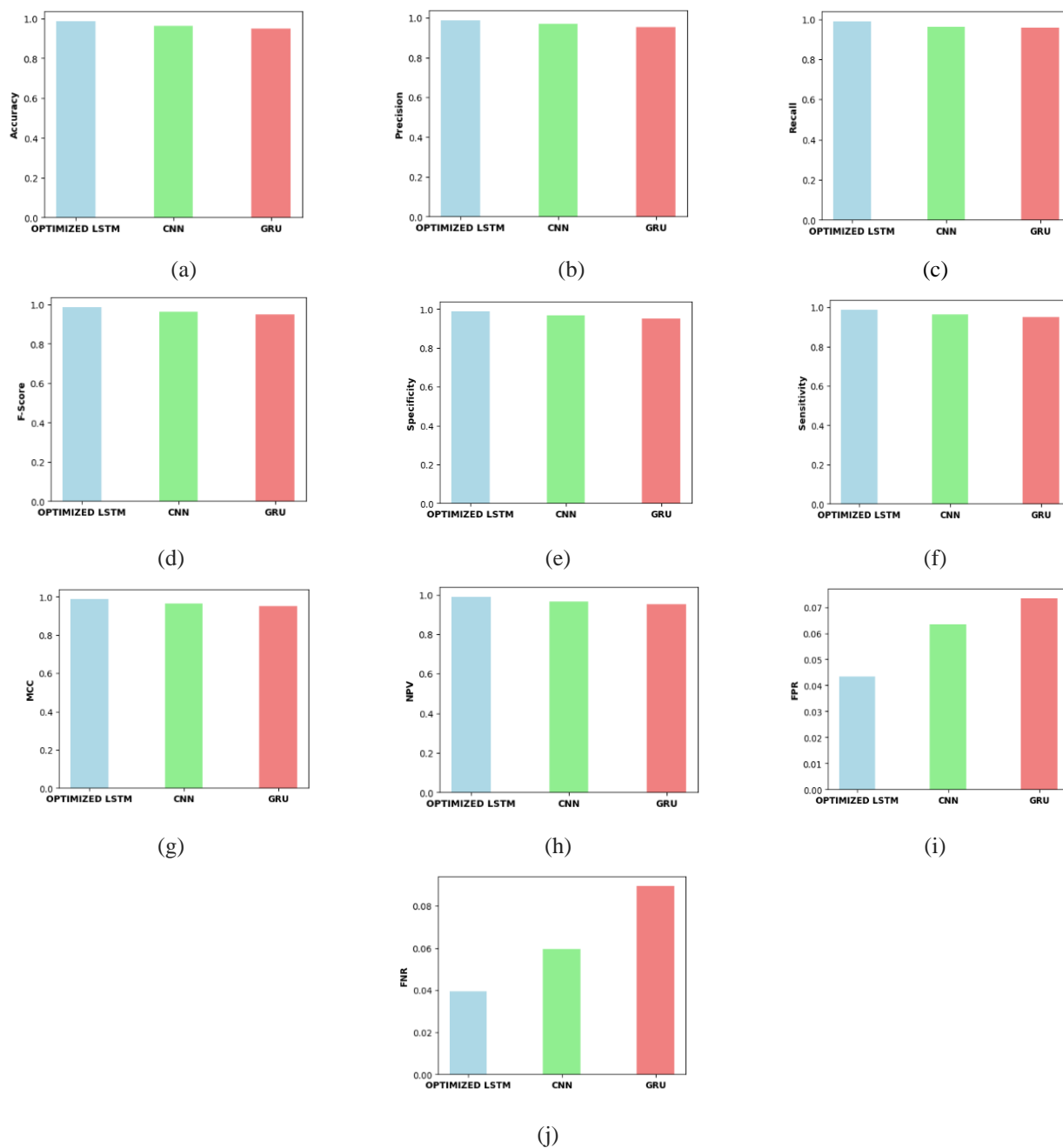


Figure 2. Classifier performance Analysis for (a) accuracy, (b) Precision, (c) Recall, (d) F_score, (e) Specificity, (f) Sensitivity, (g) MCC, (h) NPV, (i) FPR, (j) FNR

The values obtained for proposed model is related by existing techniques in Vijayvargiya et al. [16] and Vijayvargiya et al. [24] and Proposed model. The comparison is performed in terms of MAE, MSE, RMSE, correlation and MARE. The comparison is shown in table 3.

Table 3. Comparison of performance metrics for proposed model and existing techniques

| | Accuracy | Precision | Sensitivity | Specificity | F-score |
|----------------------------------|----------|-----------|-------------|-------------|---------|
| In 2022, Vijayvargiya et al.[16] | 96.69 | 96.50 | 96.62 | 98.37 | 96.55 |

| | | | | | |
|---|--------|--------|--------|-------|--------|
| In 2021, Vijayvargiya <i>et al.</i> [24] | 90.69 | 90.59 | 89.10 | 95.25 | 88.59 |
| Proposed | 98.655 | 98.712 | 98.701 | 98.8 | 98.485 |

Table 3 shows the achieved notable performance with 96.69% accuracy, exhibiting high precision (96.50%) and sensitivity (96.62%), alongside impressive specificity (98.37%) and F-score (96.55%). In 2021, a lower accuracy of 90.69% was reported, with substantial improvements observed in the proposed method, showcasing superior accuracy (98.655%) and overall performance metrics. The proposed approach demonstrates enhanced precision, sensitivity, specificity, and F-score, emphasizing its efficacy in advancing activity recognition capabilities. In Existing model Accuracy and precision are less where as in proposed model we have used advanced method and improved accuracy and other metrics. Figure 3 below depicts the classifier performance Analysis for existing model. The results highlight the significant advancements made in activity recognition through the proposed approach, setting a new standard for performance metrics in this field. These findings underscore the importance of continuous innovation and refinement in developing more accurate and effective models for activity recognition.

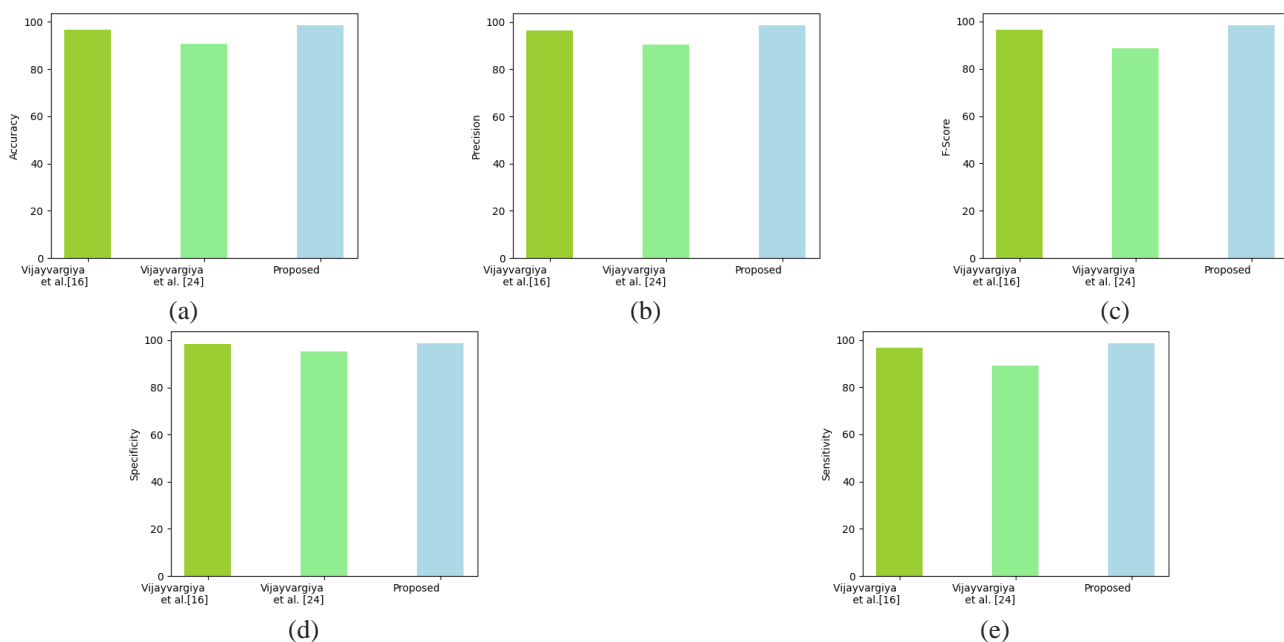


Figure 3. Classifier performance Analysis for existing model (a) accuracy, (b) Precision, (c) F_score, (d), (e) Specificity, (f) Sensitivity

5. Conclusion

The transformative role of deep learning techniques in revolutionizing lower limb prosthetics for improved activity recognition was explored. In this study, the employed approach involved the utilization of an optimized deep learning technique model to enhance the recognition of lower limb activities. The suggested methodology encompassed three key steps. The images that were gathered underwent pre-processing through the application of an enhanced wavelet denoising technique as well as Empirical mode decomposition. Subsequent to the pre-processing stage, features were extracted from the processed data by means of an enhanced sliding window approach along with a time domain feature. The extracted features were subsequently employed in the process of feature classification. The classification of the features was accomplished utilizing an Optimized LSTM model. The optimization of the LSTM model was achieved through the utilization of the black window Optimization algorithm. By calculating metrics like accuracy, precision, recall, F-score, specificity, sensitivity, MCC, NPV, FPR, FNR, the Optimized LSTM achieved higher percentages of accuracy (98.65%), precision (98.71%), sensitivity (98.70%), specificity (98.8%), and F-score (98.48%). Sustainable development principles offer a promising framework for advancing prosthetic leg innovation and improving the lives of amputees globally. Implementing advanced prosthetic technologies, such as those integrating microprocessors, neural interfaces, and advanced materials, comes with several potential challenges. By addressing the challenges through concerted efforts from researchers, healthcare providers, policymakers, and manufacturers, the benefits of

advanced prosthetic technologies can be more widely realized, improving the quality of life for individuals with limb loss. The exploring multi-modal sensor fusion, adapting models through transfer learning, integrating advanced sensors, implementing edge computing, optimizing for diverse user populations, and addressing ethical considerations for user-centric lower limb prosthetics activity recognition using deep learning.

6. Declarations

7.1. Author Contributions

Conceptualization: P.S., J.M., P.S., and M.B.; Methodology: J.M.; Software: P.S.; Validation: P.S., J.M., P.S., and M.B.; Formal Analysis: P.S., J.M., P.S., and M.B.; Investigation: P.S.; Resources: J.M.; Data Curation: J.M.; Writing Original Draft Preparation: P.S., J.M., P.S., and M.B.; Writing Review and Editing: J.M., P.S., P.S., and M.B.; Visualization: P.S.; All authors have read and agreed to the published version of the manuscript.

7.2. Data Availability Statement

The data presented in this study are available on request from the corresponding author.

7.3. Funding

The authors received no financial support for the research, authorship, and/or publication of this article.

7.4. Institutional Review Board Statement

Not applicable.

7.5. Informed Consent Statement

Not applicable.

7.6. Declaration of Competing Interest

The authors declare that they have no known competing financial interests or personal relationships that could have appeared to influence the work reported in this paper.

References

- [1] J.-H. Seo et al., "A Prosthetic Socket with Active Volume Compensation for Amputated Lower Limb," *Sensors*, vol. 21, no. 2, p. 407, Jan. 2021, doi:10.3390/s21020407.
- [2] M. Asif et al., "Advancements, Trends and Future Prospects of Lower Limb Prosthesis," *IEEE Access*, vol. 9, no. 1, pp. 85956–85977, 2021, doi: 10.1109/access.2021.3086807.
- [3] R. Bekrater-Bodmann, "Factors Associated With Prosthesis Embodiment and Its Importance for Prosthetic Satisfaction in Lower Limb Amputees," *Frontiers in Neurorobotics*, vol. 14, no. Jan., pp. 1-12, 2021, doi: 10.3389/fnbot.2020.604376.
- [4] Filippo Maria Barberi, E. Anselmino, A. Mazzoni, M. Goldfarb, and Silvestro Micera, "Toward the development of user-centered neurointegrated lower limb prostheses," *IEEE Reviews in Biomedical Engineering*, vol. 1, no. 1, pp. 1–18, Jan. 2023, doi: 10.1109/rbme.2023.3309328.
- [5] L. Qiu and M. Liu, "Innovative Design of Cultural Souvenirs Based on Deep Learning and CAD," *Computer-Aided Design and Applications*, vol. 1, no. 1, pp. 237–251, Dec. 2023, doi: 10.14733/cadaps.2024.s14.237-251
- [6] J. J. M. Driessen, M. Laffranchi, and L. De Michieli, "A reduced-order closed-loop hybrid dynamic model for design and development of lower limb prostheses," *Wearable Technologies*, vol. 4, no. 1, pp. 1-9, 2023, doi: 10.1017/wtc.2023.6.
- [7] A. das M. Silva et al., "Functional capacity of elderly with lower-limb amputation after prosthesis rehabilitation: a longitudinal study," *Disability and Rehabilitation: Assistive Technology*, vol. 1, no., 1, pp. 1–5, Nov. 2019, doi: 10.1080/17483107.2019.1684581.
- [8] L. Anojkumar, M. Ilangkumaran, and V. Sasirekha, "Comparative analysis of MCDM methods for pipe material selection in sugar industry," *Expert Systems with Applications*, vol. 41, no. 6, pp. 2964–2980, May 2014, doi: 10.1016/j.eswa.2013.10.028.
- [9] P. Qin and X. Shi, "Evaluation of Feature Extraction and Classification for Lower Limb Motion Based on sEMG Signal,"

Entropy, vol. 22, no. 8, p. 852, Jul. 2020, doi: 10.3390/e22080852.

- [10] A. Vijayvargiya, B. Singh, R. Kumar, and J. M. R. S. Tavares, "Human lower limb activity recognition techniques, databases, challenges and its applications using sEMG signal: an overview," *Biomedical Engineering Letters*, vol. 12, no. 4, pp. 343–358, Jun. 2022, doi: 10.1007/s13534-022-00236-w.
- [11] S. W. Cheatham, R. T. Baker, L. W. Larkins, J. G. Baker, and M. P. Casanova, "Clinical Practice Patterns Among Health Care Professionals for Instrument-Assisted Soft Tissue Mobilization," *Journal of Athletic Training*, vol. 56, no. 10, pp. 1100–1111, Oct. 2021, doi: 10.4085/1062-6050-047-20.
- [12] W. Chen, J. Li, S. Zhu, X. Zhang, Y. Men, and H. Wu, "Gait Recognition for Lower Limb Exoskeletons Based on Interactive Information Fusion," *Applied Bionics and Biomechanics*, vol. 2022, no. 1, pp. 1-10, Mar. 2022, doi: 10.1155/2022/9933018.
- [13] S. M. Taylor et al., "Preoperative clinical factors predict postoperative functional outcomes after major lower limb amputation: An analysis of 553 consecutive patients," *Journal of Vascular Surgery*, vol. 42, no. 2, pp. 227–234, Aug. 2005, doi: 10.1016/j.jvs.2005.04.015.
- [14] F. Peng, C. Zhang, B. Xu, J. Li, Z. Wang, and H. Su, "Locomotion Prediction for Lower Limb Prostheses in Complex Environments via sEMG and Inertial Sensors," *Complexity*, vol. 2020, pp. 1–12, Dec. 2020, doi: 10.1155/2020/8810663.
- [15] A. Vijayvargiya, B. Singh, R. Kumar, U. Desai, and J. Hemanth, "Hybrid Deep Learning Approaches for sEMG Signal-Based Lower Limb Activity Recognition," *Mathematical Problems in Engineering*, vol. 2022, no. 1, pp. 1–12, Nov. 2022, doi: 10.1155/2022/3321810.
- [16] X. Zhang and S. Tao, "Research on Pattern Recognition of Lower Limb Motion Based on Convolutional Neural Network," *Wireless Communications and Mobile Computing*, vol. 2022, no. May, pp. 1–8, May 2022, doi: 10.1155/2022/4717413.
- [17] A. Cimolato, G. Milandri, L. S. Mattos, Elena De Momi, Matteo Laffranchi, and Lorenzo De Michieli, "Hybrid Machine Learning-Neuromusculoskeletal Modeling for Control of Lower Limb Prosthetics," *2020 8th IEEE RAS/EMBS International Conference for Biomedical Robotics and Biomechanics (BioRob)*, New York, NY, USA, vol. 2020, no. Nov., pp. 557-563, Nov. 2020, doi: 10.1109/biorob49111.2020.9224448.
- [18] X. Wang et al., "sEMG-based consecutive estimation of human lower limb movement by using multi-branch neural network," *Biomedical Signal Processing and Control*, vol. 68, no. Jul., pp. 102781-102791, Jul. 2021, doi: 10.1016/j.bspc.2021.102781.
- [19] B. Zhou et al., "Accurate recognition of lower limb ambulation mode based on surface electromyography and motion data using machine learning," *Computer Methods and Programs in Biomedicine*, vol. 193, no. Sep., pp. 105486–105486, Sep. 2020, doi: 10.1016/j.cmpb.2020.105486.
- [20] T. Hussain, N. Iqbal, H. F. Maqbool, M. Khan, M. I. Awad, and A. A. Dehghani-Sani, "Intent based recognition of walking and ramp activities for amputee using sEMG based lower limb prostheses," *Biocybernetics and Biomedical Engineering*, vol. 40, no. 3, pp. 1110–1123, Jul. 2020, doi: 10.1016/j.bbe.2020.05.01.
- [21] Y. Chen, H. Jiang, C. Li, X. Jia, and P. Ghamisi, "Deep Feature Extraction and Classification of Hyperspectral Images Based on Convolutional Neural Networks," *IEEE Transactions on Geoscience and Remote Sensing*, vol. 54, no. 10, pp. 6232–6251, Oct. 2016, doi: 10.1109/tgrs.2016.258410.
- [22] J. Wang, D. Cao, J. Wang, and C. Liu, "Action Recognition of Lower Limbs Based on Surface Electromyography Weighted Feature Method," *Sensors*, vol. 21, no. 18, p. 6147, Sep. 2021, doi: 10.3390/s21186147.
- [23] Ankit Vijayvargiya, V. Gupta, R. Kumar, N. Dey, and Manuel, "A Hybrid WD-EEMD sEMG Feature Extraction Technique for Lower Limb Activity Recognition," *IEEE Sensors Journal*, vol. 21, no. 18, pp. 20431–20439, Sep. 2021, doi: 10.1109/jsen.2021.3095594.
- [24] M. Gao and G.-Y. Shi, "Ship Spatiotemporal Key Feature Point Online Extraction Based on AIS Multi-Sensor Data Using an Improved Sliding Window Algorithm," *Sensors*, vol. 19, no. 12, p. 2706, Jun. 2019, doi: 10.3390/s19122706.
- [25] I. Houamed, L. Saidi, and F. Srairi, "ECG signal denoising by fractional wavelet transform thresholding," *Research on Biomedical Engineering*, vol. 36, no. 3, pp. 349–360, Jul. 2020, doi: 10.1007/s42600-020-00075-7.
- [26] Azmi Shawkat Abdulbaqi, A. Hussein, M. Al-Juboori, Ahmed Dheyaa Radhi, Jamal Fadhil Tawfeq, and Poh Soon JosephNg, "Exploring the potential of offline cryptography techniques for securing ECG signals in healthcare," *Periodicals of engineering and natural sciences*, vol. 11, no. 3, pp. 148–148, May 2023, doi: 10.21533/pen.v11i3.3604.